

Article

Sinc Collocation Method to Simulate the Fractional Partial Integro-Differential Equation with a Weakly Singular Kernel

Mingzhu Li, Lijuan Chen * and Yongtao Zhou 

School of Science, Qingdao University of Technology, Qingdao 266525, China;
limingzhu19820120@126.com (M.L.); zhouyongtao@qut.edu.cn (Y.Z.)

* Correspondence: chenljcool@163.com

Abstract: In this article, we develop an efficient numerical scheme for dealing with fractional partial integro-differential equations (FPIEs) with a weakly singular kernel. The weight and shift Grünwald difference (WSGD) operator is adopted to approximate a time fractional derivative and the Sinc collocation method is applied for discretizing the spatial derivative. The exponential convergence of our proposed method is demonstrated in detail. Finally, numerical evidence is employed to verify the theoretical results and confirm the expected convergence rate.

Keywords: Sinc collocation method; WSGD operator; fractional partial integro-differential equation; convergence

MSC: 65M06; 65M12; 65M15



Citation: Li, M.; Chen, L.; Zhou, Y. Sinc Collocation Method to Simulate the Fractional Partial Integro-Differential Equation with a Weakly Singular Kernel. *Axioms* **2023**, *12*, 898. <https://doi.org/10.3390/axioms12090898>

Academic Editor: Chris Goodrich

Received: 1 August 2023

Revised: 11 September 2023

Accepted: 14 September 2023

Published: 21 September 2023



Copyright: © 2023 by the authors. Licensee MDPI, Basel, Switzerland. This article is an open access article distributed under the terms and conditions of the Creative Commons Attribution (CC BY) license (<https://creativecommons.org/licenses/by/4.0/>).

1. Introduction

In recent years, fractional calculus has played an increasingly important role in various fields and has attracted much interest from scholars due to its extensive applications in modeling many complex problems [1–8]. The fractional integro-differential equation is one of the most active fields in fractional calculus [9–15], which can be seen as the extension of classical integral equations by replacing integer-order derivatives with fractional derivatives. Consequently, there is a growing need to explore solution techniques to study these equations. Although there are some ways to get exact solutions of these equations, the exact solutions of these equations are very difficult to find in most cases. For this reason, there has been much research on the effective numerical methods of fractional integral differential equations (FIDEs). Here, we list only a few of them. In [16,17], the homotopy analysis method is used to find the approximate solution of FIDEs. In [18], the spectral Jacobi-collocation method is presented by Ma et al. to solve the solution of general linear FIDEs. In [19], the compact finite difference scheme is constructed to approximate the solution of FIDEs with a weakly singular kernel. In [20], the alternating direction implicit difference scheme combined with a fractional trapezoidal rule is developed to solve two dimensional FIDEs. In [21], the Legendre wavelet collocation method based on the Gauss–Jacobi quadrature is introduced to solve the fractional delay-type integro-differential equations. In [22], the collocation method combined with fractional Genocchi functions is used for the solution of variable-order FIDEs. In [23], the meshless method based on the Laplace transform is constructed for approximating the solution of the two-dimensional multi-term FIDEs. In [24], the finite element method is proposed to solve the two-dimensional weakly singular FIDEs. In [25], the spectral Galerkin method based on Legendre polynomials is presented to solve the one and two-dimensional fourth-order FIDEs. In [26], the Adomian decomposition method and homotopy perturbation method are given to approximate the solution of the time FPIEs. Liu et al. [27–31] used the multigrid method and homotopy method to solve practical problems in the fractional flow formulation of the two-phase porous media flow equations and Biot elastic models.

In this article, we consider the fractional partial integro-differential equations (FPIEs) with a weakly singular kernel as follows:

$${}_0D_t^\alpha v(x, t) = \frac{\partial^2 v(x, t)}{\partial x^2} + \int_0^t (t-s)^{-1/2} \frac{\partial^2 v(x, t)}{\partial x^2} ds + f(x, t), \quad x \in [a, b], \quad t \in [0, T], \quad (1)$$

with the initial condition:

$$v(x, 0) = 0, \quad x \in [a, b], \quad (2)$$

and boundary conditions

$$v(a, t) = v(b, t) = 0, \quad t \in [0, T], \quad (3)$$

where $0 < \alpha < 1$ and $f(x, t)$ is smooth enough. The time fractional derivative ${}_0D_t^\alpha v(x, t)$ is defined in Riemann–Liouville sense as

$${}_0D_t^\alpha v(x, t) = \frac{1}{\Gamma(1-\alpha)} \frac{d}{dt} \int_0^t \frac{v(x, s)^\alpha}{(t-s)} ds,$$

where $\Gamma(\cdot)$ is the Gamma function.

The partial integro-differential equation of integer order has proven to describe some phenomena such as viscoelasticity, population dynamics and heat conduction in materials with memory [32–34]. Over the past three decades, various numerical methods based on the Sinc approximation have been presented, which have the advantages of a very fast convergence of exponential order and handling singularities effectively. The Sinc method proposed by Frank Stenger [35–37] has been increasingly applied to solve a variety of linear and nonlinear models that arise in scientific and engineering applications such as two-point boundary value problems [38], the Blasius equation [39], oceanographic problems with boundary layers [40], fourth-order partial integro-differential equation [41], the Volterra integro-differential equation [42,43], optimal control, heat distribution and astrophysics equations. According to the definition, it can be seen that fractional derivatives and integrals always deal with weak singularities. Therefore, in the past few years, the Sinc method has been widely extended to get the numerical solution of the fractional differential equations [44–47]. The main objective of this work is to provide a new attempt to develop a numerical solution via the use of the Sinc collocation method to solve the fractional partial integro-differential equation with a weakly singular kernel.

The remainder of this article is organized as follows. In Section 2, we introduce some basic formulation and theoretic results of Sinc functions which are required for our subsequent development. In Section 3, we propose a time discrete scheme based on the weight and shift Grünwald difference operator and a space discrete scheme by applying a collocation scheme based on the Sinc functions. In Section 4, the convergence analysis of our scheme is proved and in the meantime the exponential convergence is obtained. Some numerical results are described in Section 5 to illustrate the performance of our method. Finally, we give our conclusion in Section 6.

2. Definitions and Preliminaries

In this section, we describe some main notations and definitions of the Sinc function and review some known results that will be used in the following sections. The reader interested in learning more about the detailed properties of the Sinc function can investigate [35].

The Sinc function is basically defined on the whole real line $-\infty < x < \infty$ by

$$\text{Sinc}(x) = \begin{cases} \frac{\sin(\pi x)}{\pi x}, & x \neq 0, \\ 1, & x = 0. \end{cases}$$

For any mesh size $h > 0$ and $k = 0, \pm 1, \pm 2, \dots$, the Sinc basis functions with evenly spaced nodes given on \mathbb{R} by

$$S(k, h)(x) = \text{Sinc}\left(\frac{y - kh}{h}\right).$$

Let $f(x)$ be a function defined on the real line, then for $h > 0$ the series

$$C(f, h)(x) = \sum_{k=-\infty}^{\infty} f(kh)S(k, h)(x),$$

is called the Whittaker cardinal expansion of f , whenever this series converges. The properties of Whittaker cardinal expansions which are derived on the infinite strip Q_s of the complex plane have been described and proved in detail in the literature [36].

$$Q_s = \left\{ w = t + is : |s| < d \leq \frac{\pi}{2} \right\}.$$

In order to construct approximations on the interval (a, b) , we consider the conformal map

$$\phi(z) = \log\left(\frac{z - a}{b - z}\right),$$

which carries the eye-shaped domain of complex plan

$$Q_E = \left\{ z = x + iy : \left| \arg\left(\frac{z - a}{b - z}\right) \right| < d \leq \frac{\pi}{2} \right\},$$

onto the infinite strip domain of complex plan Q_s .

Let ψ be the inverse map of $w = \phi(z)$, and we define the range of ϕ^{-1} on \mathbb{R} as

$$(a, b) = \{ \psi(u) = \phi^{-1}(u) \in Q_E : -\infty < u < \infty \}.$$

For the uniform grid $\{jh\}_{j=-\infty}^{\infty}$ on \mathbb{R} , the Sinc points which correspond to these nodes are denoted by

$$x_j = \psi(jh) = \frac{a + be^{jh}}{1 + e^{jh}}, \quad j = 0, \pm 1, \pm 2, \dots \tag{4}$$

The basis functions on (a, b) for $z \in Q_E$ are taken to be the composite translated Sinc functions as

$$S_k(z) = S(k, h) \circ \phi(z) = \text{Sinc}\left(\frac{\phi(z) - kh}{h}\right), \quad k = 0, \pm 1, \pm 2, \dots \tag{5}$$

Definition 1. Let $B(Q_E)$ be the class of functions F which are analytic in Q_E and satisfy

$$\int_{\psi(t+\Sigma)} |F(z)| dz \rightarrow 0, \quad \text{as } t \rightarrow \pm\infty,$$

where $\Sigma = \left\{ i\eta : |\eta| < d \leq \frac{\pi}{2} \right\}$ and satisfy

$$N(f) = \int_{\partial Q_E} |F(z)| dz < \infty.$$

where ∂Q_E represents the boundary of Q_E .

Lemma 1 ([37]). If $F(x), \phi'(x) \in B(Q_E)$ and $h > 0$. Let ϕ be a one-to-one conformal map. For all $x \in (a, b)$

$$\left| F(x) - \sum_{j=-N}^N F(x_j)S_j(x) \right| \leq \frac{2N(f\phi')}{\pi d} e^{-\pi d/h}. \tag{6}$$

Moreover, if $|F(x)| \leq ce^{-\beta|\phi(x)|}$, $x \in (a, b)$, for some positive constants c, l, N and β , and if the selection $h = \sqrt{\pi d / \beta N}$, then

$$\sup_{x \in (0,1)} \left| F(x) - \left(\frac{d}{dx} \right)^l \sum_{j=-N}^N f(x_j) S_j(x) \right| \leq C_1 N^{(l+1)/2} e^{-\sqrt{\pi d \beta N}}, \tag{7}$$

where C_1 depends only on F, d and β .

Lemma 1 shows the Sinc interpolation on $B(Q_E)$ is exponentially convergent. We also need the derivative of the complex Sinc function to be evaluated at the nodes. So we introduce the lemma as follows:

Lemma 2 ([48]). For the step size h and the Sinc points x_j determined by (4), suppose that ϕ is the conformal one-to-one mapping of the simply connected domain Q_E onto Q_d , then we have

$$\delta_{kj}^{(0)} = [S(k, h) \circ \phi(x)] \Big|_{x=x_j} = \begin{cases} 1, & j = k, \\ 0, & j \neq k, \end{cases} \tag{8}$$

$$\delta_{kj}^{(1)} = h \frac{d}{d\phi} [S(k, h) \circ \phi(x)] \Big|_{x=x_j} = \begin{cases} 0, & j = k, \\ \frac{(-1)^{j-k}}{j-k}, & j \neq k, \end{cases} \tag{9}$$

$$\delta_{kj}^{(2)} = h^2 \frac{d^2}{d\phi^2} [S(k, h) \circ \phi(x)] \Big|_{x=x_j} = \begin{cases} \frac{-\pi^2}{3}, & j = k, \\ \frac{-2(-1)^{j-k}}{(j-k)^2}, & j \neq k. \end{cases} \tag{10}$$

To facilitate the representation of discrete systems, we give the definition of the following matrix as follows:

$$I^{(l)} = [\delta_{kj}^{(l)}], \quad l = 0, 1, 2, \tag{11}$$

where $\delta_{kj}^{(l)}$ is the (k, j) the element of the matrix $I^{(l)}$. The matrix $I^{(0)}$, $I^{(1)}$ and $I^{(2)}$ represents the identity matrix, the skew symmetric Toeplitz matrix and the symmetric Toeplitz matrix, respectively.

3. Derivation of the Numerical Scheme

3.1. The Time Semi-Discretization

For positive integer number N , let $\tau = \frac{T}{N}$ be the time mesh size, $t_n = n\tau$, $n = 0, 1, \dots, N$, be the mesh points. Denote $v^n = v(x, t_n)$ and $f^n = f(x, t_n)$. Firstly, in order to apply the WSGD operator to discrete the time fractional derivatives, the approximation order must be used. Therefore, we review the following lemma.

Lemma 3 ([49]). Suppose that $\varphi(t) \in L_1(\mathbb{R})$ and $\varphi(t) \in C^{\alpha+1}(\mathbb{R})$, and define the shift Grünwald difference operator by

$$A_{\tau,p}^\alpha \varphi(t) = \frac{1}{\tau^\alpha} \sum_{k=0}^\infty g_k^{(\alpha)} \varphi(t - (k-p)\tau), \tag{12}$$

where p is an integer and the sequences $g_k^{(\alpha)}$ are the coefficients of the power series expansion of the function $(1-z)^\alpha$, i.e. $g_0^{(\alpha)} = 1, g_k^{(\alpha)} = (-1)^k \binom{\alpha}{k}, k = 1, 2, \dots$. Then

$$A_{\tau,p}^\alpha \varphi(t) = -\infty D_t^\alpha \varphi(t) + O(\tau), \tag{13}$$

uniformly for $t \in \mathbb{R}$ as $\tau \rightarrow 0$.

Lemma 4 ([50]). Let $\varphi(t) \in L_1(\mathbb{R})$, $-\infty D_t^{\alpha+2}\varphi(t)$ and its Fourier transform belong to $L_1(\mathbb{R})$. Define the weighted and shifted Grünwald difference operator by

$$D_{\tau,p,q}^\alpha \varphi(t) = \frac{2q - \alpha}{2(q - p)} A_{\tau,p}^\alpha \varphi(t) + \frac{2p - \alpha}{2(p - q)} A_{\tau,q}^\alpha \varphi(t), \tag{14}$$

where p and q are integers and $p \neq q$. Then,

$$D_{\tau,p,q}^\alpha \varphi(t) = -\infty D_t^\alpha \varphi(t) + O(\tau^2),$$

uniformly for $t \in \mathbb{R}$ as $\tau \rightarrow 0$.

Let p and q be equal to 0 and 1 in Lemma 4, we can get

$$\begin{aligned} {}_0D_t^\alpha v(x_i, t_n) &= \tau^{-\alpha} \left(\frac{2 + \alpha}{2} \sum_{k=0}^n g_k^{(\alpha)} v_i^{n-k} - \frac{\alpha}{2} \sum_{k=0}^{n-1} g_k^{(\alpha)} v_i^{n-1-k} \right) + O(\tau^2) \\ &= \tau^{-\alpha} \sum_{k=0}^n \lambda_k v_i^{n-k} + R_{n+1,1}, \end{aligned} \tag{15}$$

where $R_{n+1,1} = O(\tau^2)$, $\lambda_0 = \frac{2 + \alpha}{2} g_0^{(\alpha)}$, $\lambda_k = \frac{2 + \alpha}{2} g_k^{(\alpha)} - \frac{1 - \alpha}{2} g_{k-1}^{(\alpha)}$, $k \geq 1$.

By using unusual quadrature approximation, the integral term of (1) can be approximated as follows:

$$\begin{aligned} &\int_0^{t_{n+1}} (t_{n+1} - s)^{-1/2} \frac{\partial^2 v(x, s)}{\partial x^2} ds \\ &= \sum_{l=0}^n \int_{t_l}^{t_{l+1}} (t_{n+1} - s)^{-1/2} \frac{\partial^2 v(x, s)}{\partial x^2} ds \\ &\approx \sum_{l=0}^n \int_{t_l}^{t_{l+1}} (t_{n+1} - s)^{-1/2} \left(\frac{t_{l+1} - s}{\tau} v_{xx}^l(x) + \frac{s - t_l}{\tau} v_{xx}^{l+1}(x) \right) ds \\ &\approx \frac{1}{\tau} \sum_{l=0}^n \left(A_{n,l} v_{xx}^l(x) + B_{n,l} v_{xx}^{l+1}(x) \right) + R_{n+1,2}, \end{aligned} \tag{16}$$

where

$$\begin{aligned} R_{n+1,2} &= O(\Delta t^{3/2}), \\ A_{n,l} &= \int_{t_l}^{t_{l+1}} (t_{n+1} - s)^{-1/2} (t_{l+1} - s) ds, \\ B_{n,l} &= \int_{t_l}^{t_{l+1}} (t_{n+1} - s)^{-1/2} (s - t_l) ds, \end{aligned} \tag{17}$$

Substituting (15) and (16) into (1), we have

$$\begin{aligned} &\lambda_0 v^{n+1}(x) - \left(\tau^\alpha + \tau^{\alpha-1} B_{n,n} \right) v_{xx}^{n+1}(x) \\ &= \tau^{\alpha-1} \sum_{l=0}^n \rho_{n,l} v_{xx}^l(x) - \sum_{k=0}^n \lambda_k v^{n+1-k}(x) + \tau^\alpha f^{n+1}(x) + R_{n+1}, \end{aligned} \tag{18}$$

where

$$\begin{aligned} |R_{n+1}| &\leq \min \left\{ |R_{n+1,1}|, |R_{n+1,2}| \right\}, \\ \rho_{n,0} &= A_{n,0}, \\ \rho_{n,l} &= A_{n,l} + B_{n,l-1}. \end{aligned}$$

Omitting the truncation error term R_{n+1} from Equation (18), we get the following semidiscrete scheme of Equation (1):

$$\begin{aligned} & \lambda_0 v^{n+1}(x) - \left(\tau^\alpha + \tau^{\alpha-1} B_{n,n} \right) v_{xx}^{n+1}(x) \\ &= \tau^{\alpha-1} \sum_{l=0}^n \rho_{n,l} v_{xx}^l(x) - \sum_{k=0}^n \lambda_k v^{n+1-k}(x) + \tau^\alpha f^{n+1}(x), \end{aligned} \tag{19}$$

and using the initial and boundary conditions (2), we have

$$\begin{aligned} v^0(x) &= g_0(x), \\ v^{n+1}(a) &= 0, \quad v^{n+1}(b) = 0. \end{aligned}$$

3.2. The Sinc Collocation Method for Spatial Discretization

Now we construct the Sinc collocation method to discrete the semidiscrete scheme (19). The approximation solution $v^n(x)$ of the semidiscrete scheme (19) can be approximated by

$$v^n(x) \approx V_m^n(x) = \sum_{k=-N}^N c_j^n S(k, h) \circ \phi(x), \quad m = 2N + 1, \tag{20}$$

where c_j^n is the undetermined coefficient in (20).

$$\begin{aligned} \frac{d^2}{dx^2} V_m^n(x) &= \sum_{j=-N}^N c_j^n \frac{d^2}{dx^2} [S(j, h) \circ \phi(x)] \\ &= \sum_{j=-N}^N c_j^n [\phi''(x) S_j^{(1)}(x) + (\phi'(x))^2 S_j^{(2)}(x)], \end{aligned}$$

where

$$S_j^{(l)} = \frac{d^{(l)}}{d\phi^{(l)}} [S(j, h) \circ \phi(x)], \quad l = 1, 2.$$

It then follows from Lemma 2 that

$$\frac{d^2}{dx^2} V_m^n(x_i) = \sum_{j=-N}^N c_j^n \left[\phi''(x_i) \frac{\delta_{ji}^{(1)}}{h} + (\phi'(x_i))^2 \frac{\delta_{ji}^{(2)}}{h^2} \right]. \tag{21}$$

Substituting (20) and (21) into (19), we have

$$\begin{aligned} & \lambda_0 \sum_{j=-N}^{j=N} c_j^{n+1} \delta_{ji}^{(0)} - \left(\tau^\alpha + \tau^{\alpha-1} B_{n,n} \right) \sum_{j=-N}^{j=N} c_j^{n+1} \left[\phi''(x) \frac{\delta_{ji}^{(1)}}{h} + (\phi'(x))^2 \frac{\delta_{ji}^{(2)}}{h^2} \right] \\ &= \tau^{\alpha-1} \sum_{l=0}^n \sum_{j=-N}^{j=N} \rho_{n,l} c_j^{n+1} \left[\phi''(x) \frac{\delta_{ji}^{(1)}}{h} + (\phi'(x))^2 \frac{\delta_{ji}^{(2)}}{h^2} \right] \\ & \quad - \sum_{k=0}^n \sum_{j=-N}^{j=N} \lambda_k c_j^{n+1-k} \delta_{ji}^{(0)} + \tau^\alpha f_i^{n+1}. \end{aligned} \tag{22}$$

A diagonal matrix of order $2N + 1$ is defined as follows

$$D(g(x))_{ij} = \begin{cases} g(x_i), & i = j \\ 0, & i \neq j. \end{cases} \tag{23}$$

Multiplying both sides of the above equation by $\frac{1}{(\phi'(x))^2}$, we get

$$\begin{aligned} & \frac{1}{(\phi'(x_i))^2} c_i^{n+1} - (\tau^\alpha + \tau^{\alpha-1} B_{n,n}) \sum_{j=-N}^N c_j^{n+1} \left[\frac{-\phi''(x_i) \delta_{ij}^{(1)}}{(\phi'(x_i))^2 h} + \frac{\delta_{ij}^{(2)}}{h^2} \right] \\ &= \tau^{\alpha-1} \sum_{l=0}^n \sum_{j=-N}^N \rho_{n,l} c_j^l \left[\frac{-\phi''(x_i) \delta_{ij}^{(1)}}{(\phi'(x_i))^2 h} + \frac{\delta_{ij}^{(2)}}{h^2} \right] + \frac{1}{(\phi'(x_i))^2} \sum_{k=0}^n c_k^k + \frac{\tau^\alpha}{(\phi'(x_i))^2} f_i^{n+1}. \end{aligned} \tag{24}$$

Writing the above equation (24) in matrix form as

$$\begin{aligned} & D \left[\left(\frac{1}{\phi'} \right)^2 \right] C^{n+1} - (\tau^\alpha + \tau^{\alpha-1} B_{n,n}) \left[\frac{1}{h} D \left(\frac{1}{\phi'} \right)' I^{(1)} + \frac{1}{h^2} I^{(2)} \right] C^{n+1} \\ &= \tau^\alpha D \left[\left(\frac{1}{\phi'} \right)^2 \right] F^{n+1} + D \left[\left(\frac{1}{\phi'} \right)^2 \right] (C^n + C^{n-1} + \dots + C^1 + C^0) \\ &+ \tau^{\alpha-1} \sum_{l=0}^n \rho_{n,l} \left[\frac{1}{h} D \left(\frac{1}{\phi'} \right)' I^{(1)} + \frac{1}{h^2} I^{(2)} \right] C^l, \end{aligned} \tag{25}$$

or in a compact form as

$$PC^{n+1} = R \left(\tau^\alpha F^{n+1} + \sum_{m=0}^n C^m \right) + \tau^{\alpha-1} \sum_{l=0}^n \rho_{n,l} QC^l, \tag{26}$$

where

$$\begin{aligned} R &= D \left[\left(\frac{1}{\phi'} \right)^2 \right], \\ Q &= \frac{1}{h} D \left(\frac{1}{\phi'} \right)' I^{(1)} + \frac{1}{h^2} I^{(2)}, \\ C^{n+1} &= (c_{-N}^{n+1}, c_{-N+1}^{n+1}, \dots, c_N^{n+1})^T, \\ F^{n+1} &= (f_{-N}^{n+1}, f_{-N+1}^{n+1}, \dots, f_N^{n+1})^T, \\ P &= R - B_{n,n}Q. \end{aligned} \tag{27}$$

If we set

$$G^{n+1} = R \left(\tau^\alpha F^{n+1} + \sum_{m=0}^n C^m \right) + \tau^{\alpha-1} \sum_{l=0}^n \rho_{n,l} QC^l,$$

then Equation (26) can be written as follows:

$$PC^{n+1} = G^{n+1}, \tag{28}$$

with the additional initial condition

$$C^0 = (V_0(x_{-N}), V_0(x_{-N+1}), \dots, V_0(x_N))^T.$$

For each n , Formula (28) is a system of $2N + 1$ order linear equations including $2N + 1$ equations. By solving this system of linear equations, the coefficients of the numerical solutions (20) can be obtained.

4. Convergence Analysis

In this section, we aim to analyze the convergence of the semidiscrete Equation (19) for the FPIEs (1)–(3).

For the sake of convenience, the semidiscrete Equation (19) can be rewritten as

$$\lambda_0 v^{n+1}(x) - (\tau^\alpha + \tau^{\alpha-1} B_{n,n}) v_{xx}^{n+1}(x) = g(x), \tag{29}$$

where

$$g(x) = \tau^{\alpha-1} \sum_{l=0}^n \rho_{n,l} v_{xx}^l(x) - \sum_{k=0}^n \lambda_k v^{n+1-k}(x) + \tau^\alpha f^{n+1}(x).$$

The numerical solution $W_m^{n+1}(x)$ of Equation (29) at the point x_j can be obtained by

$$W_m^{n+1}(x) = \sum_{j=-N}^N v^{n+1}(x_j) S_j(x), \tag{30}$$

To obtain the bound of $|V^{n+1}(x) - W_m^{n+1}(x)|$, we can start by estimating the boundary of $|V_m^{n+1}(x) - W_m^{n+1}(x)|$.

Lemma 5 ([51]). For $x \in \phi^{-1}$ and the matrix P defined by Equation (27), we have

$$\frac{P + P^*}{2} = H - \frac{B_{n,n}}{h^2} I^{(2)},$$

where P^* is the conjugate transpose of P and

$$H = D \left[\operatorname{Re} \left(\left(\frac{1}{\phi'} \right)^2 \right) \right] - \frac{B_{n,n}}{2h} \left\{ D \left[\left(\frac{1}{\phi'} \right)' \right] I^{(1)} - I^{(1)} D \left[\left(\frac{1}{\phi'} \right)' \right] \right\}.$$

If the eigenvalues of the matrix H are non-negative, then there exists a constant c_0 that doesn't depend on N , such that

$$\|P^{-1}\|_2 \leq \frac{4dN}{\beta\pi B_{n,n}} \left(1 + \frac{C_0}{N} \right),$$

for a sufficiently large N .

Theorem 1. Suppose $V_m^{n+1}(x)$ is an approximate solution of Equation (19), W_m^{n+1} is an approximate solution of Equation (1). Then, there exists a constant C_4 that doesn't depend on N , such that

$$\sup_{x \in [a,b]} |V_m^{n+1}(x) - W_m^{n+1}(x)| \leq C_4 N^3 e^{-\sqrt{\pi d \beta N}}.$$

Proof. By Equations (20) and (30) and the Cauchy–Schwarz inequality, we gain

$$\begin{aligned} |V_m^{n+1}(x) - W_m^{n+1}(x)| &= \left| \sum_{j=-N}^N c_j^{n+1} S_j(x) - \sum_{j=-N}^N v^{n+1}(x_j) S_j(x) \right| \\ &\leq \left(\sum_{j=-N}^N |c_j^{n+1} - v^{n+1}(x_j)|^2 \right)^{\frac{1}{2}} \left(\sum_{j=-N}^N |S_j(x)|^2 \right)^{\frac{1}{2}}. \end{aligned} \tag{31}$$

Since $\left(\sum_{j=-N}^N |S_j(x)|^2 \right)^{\frac{1}{2}} \leq C_1$, where C_1 is a constant independent of N , we obtain

$$|V_m^{n+1}(x) - W_m^{n+1}(x)| \leq C_1 \|C^{n+1} - U^{n+1}\|_2, \tag{32}$$

where C^{n+1} is given by (27) and denoting the vector V^{n+1} by

$$U^{n+1} = \left(v^{n+1}(x_{-N}), v^{n+1}(x_{-N+1}), \dots, v^{n+1}(x_N) \right)^T.$$

Based on (19) and (28), we have

$$\|C^{n+1} - U^{n+1}\|_2 = \|P^{-1}(PC^{n+1} - PU^{n+1})\|_2 \leq \|P^{-1}\|_2 \|PU^{n+1} - G^{n+1}\|_2. \tag{33}$$

For simplicity, we denote

$$r_k = (PU^{n+1} - G^{n+1})_k, \quad k = -N, \dots, N,$$

and using Equation (29), we obtain

$$\begin{aligned} |r_k| &= |g(x_k) - g_m(x_k)| \\ &= \left| v^{n+1}(x_k) - \left(\tau^\alpha + \tau^{\alpha-1}B_{n,n}\right) \frac{d^2}{dx^2} v^{n+1}(x_k) - V_m^{n+1}(x_k) + \left(\tau^\alpha + \tau^{\alpha-1}B_{n,n}\right) \frac{d^2}{dx^2} V_m^{n+1}(x_k) \right| \\ &\leq |v^{n+1}(x_k) - V_m^{n+1}(x_k)| + B_{n,n} \left| \frac{d^2}{dx^2} v^{n+1}(x_k) - \frac{d^2}{dx^2} V_m^{n+1}(x_k) \right|. \end{aligned} \tag{34}$$

Now, using Theorem 1, we have

$$\begin{aligned} \|r_k\| &\leq C_2 N^{\frac{1}{2}} e^{-\sqrt{\pi d \beta N}} + B_{n,n} C_3 N^{\frac{3}{2}} e^{-\sqrt{\pi d \beta N}} \\ &\leq e^{-\sqrt{\pi d \beta N}} \left(C_2 N^{\frac{3}{2}} + B_{n,n} C_3 N^{\frac{3}{2}} \right) \\ &= KN^{\frac{3}{2}} e^{-\sqrt{\pi d \beta N}}, \end{aligned} \tag{35}$$

where C_2 and C_3 are constants independent of N and $K = C_2 + B_{n,n}C_3$.

$$\|PU^{n+1} - G^{n+1}\|_2 \leq \sqrt{2N+1} \|PU^{n+1} - G^{n+1}\|_\infty,$$

and using inequality (35), we get

$$\|PU^{n+1} - G^{n+1}\|_2 \leq \sqrt{2}KN^2 e^{-\sqrt{\pi d \beta N}}. \tag{36}$$

Now, substituting (36) into (33), we have

$$\|C^{n+1} - U^{n+1}\|_2 \leq \frac{4\sqrt{2}dK(1 + C_0)}{\alpha\pi B_{n,n}} N^3 e^{-\sqrt{\pi d \beta N}}. \tag{37}$$

Based on (32) and (37), we get

$$\sup_{x \in [a,b]} |V_m^{n+1}(x) - W_m^{n+1}(x)| \leq C_4 N^3 e^{-\sqrt{\pi d \beta N}}, \tag{38}$$

where $C_4 = \frac{4\sqrt{2}dK(1 + C_0)}{\alpha\pi B_{n,n}}$. \square

Theorem 2. Suppose $V^{n+1}(x)$ be the analytical solution of (29), $V_m^{n+1}(x)$ be its Sinc approximation defined by (20). Then, there exists a constant C_7 that doesn't depend on N , such that

$$\sup_{x \in [a,b]} |V^{n+1}(x) - V_m^{n+1}(x)| \leq C_7 N^3 e^{-\sqrt{\pi d \beta N}}.$$

Proof. Using the triangular inequality, we get

$$|V^{n+1}(x) - V_m^{n+1}(x)| \leq |V^{n+1}(x) - W_m^{n+1}(x)| + |W_m^{n+1}(x) - V_m^{n+1}(x)|. \tag{39}$$

Using Theorem 1, we can get

$$|V^{n+1}(x) - W_m^{n+1}(x)| \leq C_5 N^3 e^{-\sqrt{\pi d \beta N}}. \tag{40}$$

where C_5 is a constant independent of N . Based on Theorem 2, there exists a constant C_6 that does not depend on N such that

$$|W_m^{n+1}(x) - V_m^{n+1}(x)| \leq C_6 N^3 e^{-\sqrt{\pi d \beta N}}, \tag{41}$$

Finally, we conclude

$$\sup_{x \in [a,b]} |V^{n+1}(x) - V_m^{n+1}(x)| \leq C_7 N^3 e^{-\sqrt{\pi d \beta N}}, \tag{42}$$

where $C_7 = \max\{C_5, C_6\}$. \square

5. Numerical Results

In this section, some numerical calculations are performed to demonstrate the validity and accuracy of our method. In numerical examples, we set parameters $d = \frac{\pi}{2}$ and $\beta = 1$ and then $h = \frac{\pi}{\sqrt{2N}}$. All numerical computations are carried out using Matlab 7.14 running on a Lenovo PC (Lenovo, Quarry Bay, Hong Kong) with a 1.6 GHz Intel Core i5-4200 CPU (Intel Corporation, Santa Clara, CA, USA) and 4 GB RAM installed.

To illustrate the accuracy of our method, the error analysis is calculated according to the maximum norm errors, defined as:

$$e_\infty(h, \tau) = \max_{0 \leq n \leq N} \|V^n - v^n\|_\infty.$$

Furthermore, the temporal convergence order can be expressed by

$$rate_1 = \log_2 \left(\frac{e_\infty(h, 2\tau)}{e_\infty(h, \tau)} \right).$$

Example 1. We consider Equations (1)–(3) with the analytical solution

$$v(x, t) = t^2 x(x - 1),$$

where $0 < x < 1, 0 < t < 1$ and

$$f(x, t) = \frac{2}{\Gamma(3 - \alpha)} x(x - 1)t^{2-\alpha} - 2t^2 - \frac{4\Gamma(1/2)}{\Gamma(7/2)} t^{\frac{5}{2}}.$$

Table 1 represents the maximum norm errors and the temporal convergence order for $N = 32$ and $\alpha = 0.1, 0.3, 0.5, 0.7$ with different values of time step size. Table 2 shows a comparative study for the presented method and the method in [19]. It can be observed from the table that the numerical results are better than the method in [19]. The maximum norm errors for $\alpha = 0.8$ and $\tau = \frac{1}{1000}$ with different values of N are plotted in Figure 1. At the same time, it is clear from the figure that the presented scheme converges at an exponential rate as N increases. From these diagrams, it can be seen that the results are in excellent agreement with the theoretical analysis.

Table 1. The maximum norm errors and temporal convergence orders with $N = 32$.

| α | τ | $e_\infty(h, \tau)$ | $Rate_1$ |
|----------|--------|--------------------------|----------|
| 0.1 | 1/10 | 2.71422×10^{-4} | * |
| | 1/20 | 6.89322×10^{-5} | 1.97729 |
| | 1/40 | 1.74371×10^{-5} | 1.98507 |
| | 1/80 | 4.40355×10^{-6} | 1.98542 |
| 0.3 | 1/10 | 2.71798×10^{-4} | * |
| | 1/20 | 6.90718×10^{-5} | 1.97637 |
| | 1/40 | 1.74383×10^{-5} | 1.98584 |
| | 1/80 | 4.41692×10^{-6} | 1.98115 |
| 0.5 | 1/10 | 2.78117×10^{-4} | * |
| | 1/20 | 7.06728×10^{-5} | 1.97647 |
| | 1/40 | 1.78836×10^{-5} | 1.98252 |
| | 1/80 | 4.51750×10^{-6} | 1.98504 |
| 0.7 | 1/10 | 2.90936×10^{-4} | * |
| | 1/20 | 7.37990×10^{-5} | 1.97903 |
| | 1/40 | 1.86602×10^{-5} | 1.98365 |
| | 1/80 | 4.71342×10^{-6} | 1.98512 |

The asterisk (*) symbol indicates that the temporal convergence order cannot be calculated.

Table 2. Comparison of the maximum norm errors and temporal convergence orders with $N = 100$.

| α | τ | $e_\infty(h, \tau)$ | $Rate_1$ | $e_\infty(h, \tau)$ [19] | $Rate_1$ [19] |
|----------|--------|-------------------------|----------|--------------------------|---------------|
| 0.6 | 1/10 | 2.7821×10^{-4} | * | 2.4541×10^{-4} | * |
| | 1/20 | 7.0565×10^{-5} | 1.9791 | 9.4738×10^{-5} | 1.3732 |
| | 1/40 | 1.7991×10^{-5} | 1.9717 | 3.8919×10^{-5} | 1.2835 |
| | 1/80 | 4.5933×10^{-6} | 1.9696 | 1.6656×10^{-5} | 1.2244 |
| | 1/160 | 1.1502×10^{-6} | 1.9976 | 7.3463×10^{-6} | 1.1810 |
| | 1/320 | 2.8781×10^{-7} | 1.9987 | 3.3191×10^{-6} | 1.1462 |

The asterisk (*) symbol indicates that the temporal convergence order cannot be calculated.

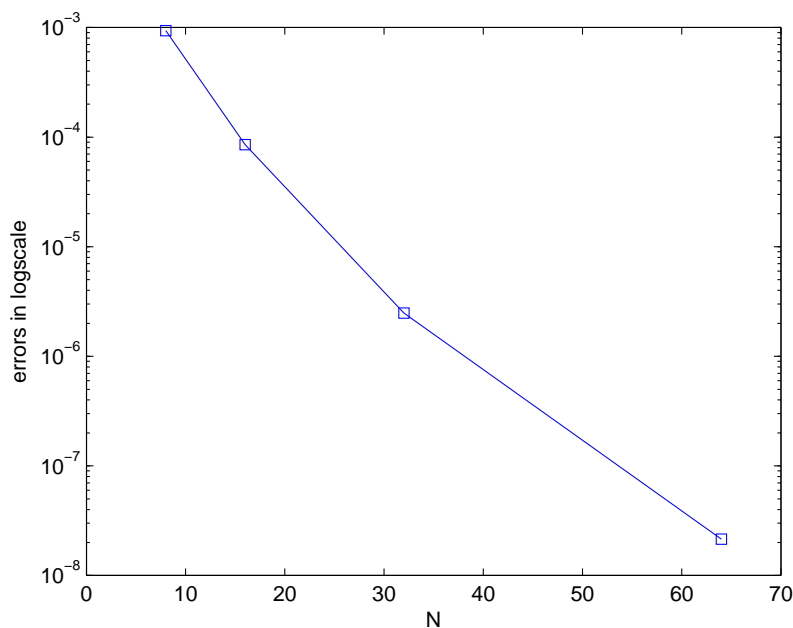


Figure 1. The maximum norm errors with $\alpha = 0.8$ and $\tau = \frac{1}{1000}$.

Example 2. We consider Equations (1)–(3) with the analytical solution

$$v(x, t) = t \sin(\pi x),$$

where $0 < x < \pi, 0 < t < 1$ and

$$f(x, t) = \sin(\pi x) \left(\frac{1}{\Gamma(2 - \alpha)} t^{1-\alpha} + \pi^2 t + \frac{4}{3} \pi^2 t^{\frac{3}{2}} \right).$$

Table 3 represents the maximum norm errors and the temporal convergence order for $N = 128$ and $\alpha = 0.2, 0.4, 0.6, 0.8$ with different values of time step size. The maximum norm errors for $\alpha = 0.4$ and $\tau = \frac{1}{512}$ with different values of N are plotted in Figure 2. The figure also shows that our presented scheme converges at an exponential rate as N increases. Figure 3 depicts the graph of the numerical solution and the exact solution with $\alpha = 0.5, \tau = \frac{1}{512}$ and $N = 64$. These figures confirm that the proposed method solution is in good agreement with the exact solution.

Table 3. The maximum norm errors and temporal convergence orders with $N = 128$.

| α | τ | $e_{\infty}(h, \tau)$ | $Rate_1$ |
|----------|--------|-------------------------|----------|
| 0.2 | 1/10 | 1.4168×10^{-6} | * |
| | 1/20 | 3.5892×10^{-7} | 1.9809 |
| | 1/40 | 9.0501×10^{-8} | 1.9877 |
| | 1/80 | 2.2729×10^{-8} | 1.9934 |
| 0.4 | 1/10 | 6.0618×10^{-6} | * |
| | 1/20 | 1.5345×10^{-6} | 1.9819 |
| | 1/40 | 3.8691×10^{-7} | 1.9877 |
| | 1/80 | 9.7218×10^{-8} | 1.9918 |
| 0.6 | 1/10 | 2.1210×10^{-5} | * |
| | 1/20 | 5.3633×10^{-6} | 1.9836 |
| | 1/40 | 1.3508×10^{-6} | 1.9894 |
| | 1/80 | 3.3889×10^{-7} | 1.9949 |
| 0.8 | 1/10 | 6.8883×10^{-5} | * |
| | 1/20 | 1.7426×10^{-5} | 1.9829 |
| | 1/40 | 4.3913×10^{-6} | 1.9885 |
| | 1/80 | 1.1017×10^{-6} | 1.9949 |

The asterisk (*) symbol indicates that the temporal convergence order cannot be calculated.

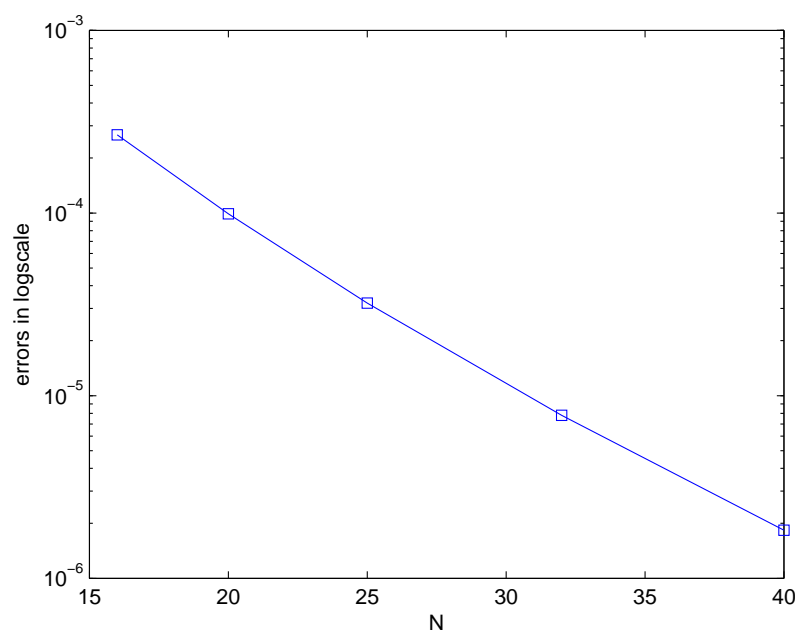


Figure 2. The maximum norm errors with $\alpha = 0.4$ and $\tau = \frac{1}{512}$.

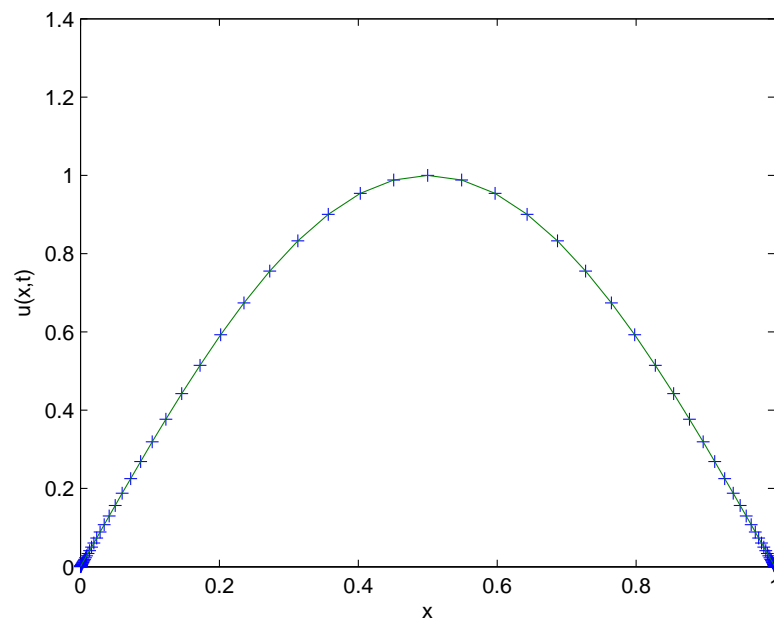


Figure 3. Numerical solution and analytical solution with $\alpha = 0.5$, $\tau = \frac{1}{512}$ and $N = 64$.

6. Conclusions

In the present article, we have presented and analyzed an efficient numerical algorithm for solving FPIEs with a weakly singular kernel. In this technique, the WSGD operator is applied for discretization of the time fractional derivative and the Sinc collocation method is used for discretization of the space derivative. Convergence analysis of our scheme is theoretically proven, and it is shown that the numerical solution converges to the exact solution at the exponential rate in space. Numerical experiments were provided to verify the theoretical results. In the future, we intend to extend the method for solving the higher space dimension equation, which is straightforward, in view of the potential applications.

Author Contributions: Conceptualization, M.L. and L.C.; methodology, M.L. and L.C.; validation, L.C. and Y.Z.; writing—original draft preparation, M.L. and Y.Z.; writing—review and editing, M.L. and Y.Z.; funding acquisition, M.L. and L.C. All authors have read and agreed to the published version of the manuscript.

Funding: This research was supported by the Natural Science Foundation of Shandong Province under Grant ZR2022MA063 and the National Natural Science Foundation of China under Grant 12101037.

Data Availability Statement: Not applicable.

Conflicts of Interest: The authors declare no conflict of interest.

References

- Hilfer, R. *Applications of Fractional Calculus in Physics*; World Scientific: Singapore, 2000.
- Podlubny, I. *Fractional Differential Equations*; Academic Press: San Diego, CA, USA, 1999.
- Povstenko, Y. *Fractional Thermoelasticity*; Springer: New York, NY, USA, 2015.
- Cheng, X.; Duan, J.; Li, D. A novel compact ADI scheme for two-dimensional Riesz space fractional nonlinear reaction-diffusion equations. *Appl. Math. Comput.* **2019**, *346*, 452–464. [[CrossRef](#)]
- Yousuf, M.; Furati, K. M.; Khaliq, A.Q.M. High-order time-stepping methods for two-dimensional Riesz fractional nonlinear reaction-diffusion equations. *Comput. Math. Appl.* **2020**, *80*, 204–226. [[CrossRef](#)]
- Yousuf, M. A second-order efficient L-stable numerical method for space fractional reaction-diffusion equations. *Int. J. Comput. Math* **2018**, *95*, 1408–1422. [[CrossRef](#)]
- El-Danaf, T.S.; Hadhoud, A.R. Parametric spline functions for the solution of the one time fractional Burgers' equation. *Appl. Math. Model.* **2012**, *36*, 4557–4564. [[CrossRef](#)]
- El-Danaf, T.S.; Hadhoud, A.R. Computational method for solving space fractional Fisher's nonlinear equation. *Math. Methods Appl. Sci.* **2014**, *37*, 657–662. [[CrossRef](#)]

9. Panda, R.; Dash, M. Fractional generalized splines and signal processing. *Signal Process.* **2006**, *86*, 2340–2350. [[CrossRef](#)]
10. Torvik, P.J.; Bagley, R.L. On the appearance of the fractional derivative in the behavior of real materials. *J. Appl. Mech.* **1984**, *51*, 294–298. [[CrossRef](#)]
11. Giona, M.; Cerbelli, S.; Roman, H.E. Fractional diffusion equation and relaxation in complex viscoelastic material. *Phys. A* **1992**, *191*, 449–453. [[CrossRef](#)]
12. Jiang, X.; Xu, M.; Qi, H. The fractional diffusion model with an absorption term and modified Fick's law for non-local transport processes. *Nonlinear Anal.* **2010**, *11*, 262–269. [[CrossRef](#)]
13. Monami, S.; Odibat, Z. Analytical approach to linear fractional partial differential equations arising in fluid mechanics. *Phys. Lett. A* **2006**, *355*, 271–279.
14. He, J.H. Some applications of nonlinear fractional differential equations and their approximations. *Bull. Sci. Technol.* **1999**, *15*, 86–90.
15. Chow, T. Fractional dynamics of interfaces between soft-nanoparticles and rough substrates. *Phys. Lett.* **2005**, *342*, 148–155. [[CrossRef](#)]
16. Yildirim, A.; Sezer, S.A.; Kaplan, Y. Numerical methods for fourth-order fractional integro-differential equations. *Z. Naturforsch. A* **2011**, *65*, 1027–1032. [[CrossRef](#)]
17. Abbasbandy, S.; Hashemi, M.S.; Hashim, I. On convergence of homotopy analysis method and its application to fractional integro-differential equations. *Quaest. Math.* **2013**, *36*, 93–105. [[CrossRef](#)]
18. Ma, X.; Huang, C. Spectral collocation method for linear fractional integro-differential equations. *Appl. Math. Model.* **2014**, *38*, 1434–1448. [[CrossRef](#)]
19. Mohebbi, A. Compact finite difference scheme for the solution of a time fractional partial integro-differential equation with a weakly singular kernel. *Math. Methods Appl. Sci.* **2017**, *40*, 7627–7639. [[CrossRef](#)]
20. Qiao, L.; Xu, D.; Wang, Z. An ADI difference scheme based on fractional trapezoidal rule for fractional integro-differential equation with a weakly singular kernel. *Appl. Math. Comput.* **2019**, *354*, 103–114. [[CrossRef](#)]
21. Nemati, S.; Lima, P.M.; Sedaghat, S. Legendre wavelet collocation method combined with the Gauss-Jacobi quadrature for solving fractional delay-type integro-differential equations. *Appl. Numer. Math.* **2020**, *149*, 99–112. [[CrossRef](#)]
22. Dehestani, H.; Ordokhani, Y.; Razzaghi, M. Pseudo-operational matrix method for the solution of variable-order fractional partial integro-differential equation. *Eng. Comput.* **2021**, *37*, 1791–1806. [[CrossRef](#)]
23. Kamran, K.; Shah, Z.; Kumam, P.; Alreshidi, N.A. A meshless method based on the Laplace transform for the 2D multi-term time fractional partial integro-differential equation. *Mathematics* **2020**, *8*, 1972. [[CrossRef](#)]
24. Dehghan, M.; Abbaszadeh, M. Error estimate of finite element/finite difference technique for solution of two-dimensional weakly singular integro-partial differential equation with space and time fractional derivative. *Appl. Numer. Math.* **2019**, *356*, 314–328. [[CrossRef](#)]
25. Fakhar-Izadi, F. Fully spectral-Galerkin method for the one and two dimensional fourth order time fractional partial integro-differential equations with a weakly singular kernel. *J. Numer. Methods Partial Differ. Equ.* **2022**, *38*, 160–176. [[CrossRef](#)]
26. Panda, A.; Santra, S.; Mohapatra, J. Adomian decomposition and homotopy perturbation method for the solution of time fractional partial integro-differential equations. *J. Appl. Math. Comput.* **2022**, *68*, 2065–2082. [[CrossRef](#)]
27. Liu, T.; Ouyang, D.; Guo, L.; Qiu, R.; Qi, Y.; Xie, W.; Ma, Q.; Liu, C. Combination of multigrid with constraint data for inverse problem of nonlinear diffusion equation. *Mathematics* **2023**, *11*, 2887. [[CrossRef](#)]
28. Liu, T. Parameter estimation with the multigrid-homotopy method for a nonlinear diffusion equation. *J. Comput. Appl. Math.* **2022**, *413*, 114393. [[CrossRef](#)]
29. Liu, T. Porosity reconstruction based on Biot elastic model of porous media by homotopy perturbation method. *Chaos Solitons Fractals* **2022**, *158*, 112007. [[CrossRef](#)]
30. Liu, T.; Ding, Z.; Yu, J.; Zhang, W. Parameter estimation for nonlinear diffusion problems by the constrained homotopy method. *Mathematics* **2023**, *11*, 2642. [[CrossRef](#)]
31. Liu, T.; Xia, K.; Zheng, Y.; Yang, Y.; Qiu, R.; Qi, Y.; Liu, C. A homotopy method for the constrained inverse problem in the multiphase porous media flow. *Processes* **2022**, *10*, 1143. [[CrossRef](#)]
32. Tuan, V.K. Fractional partial integro-differential equation in wiener spaces. *Fract. Calc. Appl. Anal.* **2020**, *23*, 1300–1328. [[CrossRef](#)]
33. Zhu, B.; Han, B.Y. Existence and uniqueness of mild solutions for fractional partial integro-differential equations. *Mediterr. J. Math.* **2020**, *17*, 113. [[CrossRef](#)]
34. Maji, S.; Natesan, S. Analytical and numerical solution techniques for a class of time-fractional integro-partial differential equations. *Numer. Algorithms* **2023**, *94*, 229–256. [[CrossRef](#)]
35. Stenger, B.F. Numerical methods based on the Whittaker cardinal or Sinc functions. *SIAM Rev.* **1981**, *23*, 165–224. [[CrossRef](#)]
36. Stenger, B.F. Sinc Methods for Quadrature and Differential Equations. *SIAM Rev.* **1993**, *35*, 682–683. [[CrossRef](#)]
37. Stenger, B.F. *Numerical Methods Based on Sinc and Analytic Functions*; Springer: New York, NY, USA, 1993.
38. Rashidinia, J.; Nabati, M.; Barati, A. Sinc-Galerkin method for solving nonlinear weakly singular two point boundary value problems. *Int. J. Comput. Math.* **2017**, *94*, 79–94. [[CrossRef](#)]
39. Parand, K.; Dehghan, M.; Pirkhedri, A. Sinc-collocation method for solving the Blasius equation. *Phys. Lett. A* **2009**, *373*, 4060–4065. [[CrossRef](#)]

40. Winter, D.F.; Bowers, K.; Lund, J. Wind-driven currents in a sea with a variable Eddy viscosity calculated via a Sinc–Galerkin technique. *Int. J. Numer. Methods Fluids* **2000**, *33*, 1041–1073. [[CrossRef](#)]
41. Qiu, W.; Xu, D.; Guo, J. The Crank-Nicolson-type Sinc-Galerkin method for the fourth-order partial integro-differential equation with a weakly singular kernel. *Appl. Numer. Math.* **2021**, *159*, 239–258. [[CrossRef](#)]
42. Okayama, K. Theoretical analysis of a Sinc-Nyström method for Volterra integro-differential equations and its improvement. *Appl. Math. Comput.* **2018**, *324*, 1–15. [[CrossRef](#)]
43. Al-Khaled, K.; Darweesh, A.; Yousef, M.H. Convergence of numerical scheme for the solution of partial integro-differential equations used in heat transfer. *J. Appl. Math. Comput.* **2019**, *61*, 657–675. [[CrossRef](#)]
44. Nagy, A.M. Numerical solution of time fractional nonlinear Klein–Gordon equation using Sinc-Chebyshev collocation method. *Appl. Math. Comput.* **2017**, *310*, 139–148. [[CrossRef](#)]
45. Saadatmandi, A.; Dehghan, M.; Azizi, M. The Sinc-Legendre collocation method for a class of fractional convection-diffusion equations with variable coefficients. *Commun. Nonlinear Sci. Numer. Simul.* **2012**, *17*, 4125–4136. [[CrossRef](#)]
46. Pirkhedri, A.; Javadi, H.H.S. Solving the time-fractional diffusion equation via Sinc-Haar collocation method. *Appl. Math. Comput.* **2015**, *257*, 317–326. [[CrossRef](#)]
47. Chen, L.; Li, M.; Xu, Q. Sinc-Galerkin method for solving the time fractional convection–diffusion equation with variable coefficients. *Adv. Differ. Equ.* **2020**, *2020*, 504. [[CrossRef](#)]
48. Lund, J.; Bowers, K. *Sinc Method for Quadrature and Differential Equations*; SIAM: Philadelphia, PA, USA, 1992.
49. Meerschaert, M.M.; Tadjeran, C. Finite difference approximations for fractional advection dispersion flow equations. *J. Comput. Appl. Math.* **2004**, *172*, 65–77. [[CrossRef](#)]
50. Tian, W.Y.; Zhou, H.; Deng, W.H. A class of second order difference approximations for solving space fractional diffusion equations. *Math. Comput.* **2015**, *84*, 1703–1727. [[CrossRef](#)]
51. Fahim, A.; Araghi, M.A.F.; Rashidinia, J.; Jalalvand, M. Numerical solution of Volterra partial integro-differential equations based on Sinc-collocation method. *Adv. Differ. Equ.* **2017**, *2017*, 362. [[CrossRef](#)]

Disclaimer/Publisher’s Note: The statements, opinions and data contained in all publications are solely those of the individual author(s) and contributor(s) and not of MDPI and/or the editor(s). MDPI and/or the editor(s) disclaim responsibility for any injury to people or property resulting from any ideas, methods, instructions or products referred to in the content.